AAEC/E322

AAEC/E322

(1)

AUSTRALIAN ATOMIC ENERGY COMMISSION

RESEARCH ESTABLISHMENT

LUCAS HEIGHTS

METHYL IODIDE PENETRATION OF CHARCOAL BEDS: VARIATION WITH RELATIVE HUMIDITY AND FACE VELOCITY

by

F. G. MAY

H. J. POLSON

September 1974

ISBN 0 642 99653 9

AUSTRALIAN ATOMIC ENERGY COMMISSION
RESEARCH ESTABLISHMENT
LUCAS HEIGHTS

METHYL IODIDE PENETRATION OF CHARCOAL BEDS: VARIATION WITH RELATIVE HUMIDITY AND FACE VELOCITY

by

F.G. MAY
H.J. POLSON

ABSTRACT

The retention of methyl iodide in charcoal beds was found to vary with the distance from the leading edges of the beds. Near the leading edges, retention was less than in the deeper regions, probably due to the chemisorption of competing vapours in the airstream drawn through the beds. One of the poisoning agents was identified as di-methyl sulphate vapour. The penetration of methyl iodide fell exponentially with distance in the deeper regions of the beds. The slope of the penetration curves in these deeper regions was dependent on the relative humidity and the face velocity in a more complex manner than the simple relationship assumed in the 'Stay Time'

(Continued)

concept. An empirical formula, which gave the slope of the penetration curve within a standard deviation of 7 per cent, was derived to correlate the parameters over the range of practical interest, *i.e.* 30-99 per cent relative humidity and from 1.1 m s^{-1} down to at least 0.16 m s^{-1}, and probably much lower. The uncertainty in the results could have been caused by variations within the batches of charcoal.

A formula was derived to translate the results of an *in situ* test at a measured flowrate and humidity into an expected performance at high humidity and any other flowrate. The expression is independent of the slope of the penetration curve and the thicknesses of both the poisoned and unpoisoned regions of the bed, which suggests that it may be valid even for heavily poisoned beds.

National Library of Australia card number and ISBN 0 642 99653 9

The following descriptors have been selected from the INIS Thesaurus to describe the subject content of this report for information retrieval purposes. For further details please refer to IAEA–INIS–12 (INIS: Manual for Indexing) and IAEA–INIS–13 (INIS: Thesaurus) published in Vienna by the International Atomic Energy Agency.

AIR FILTERS; CHARCOAL; CHEMISORPTION; FLOW RATE; HUMIDITY; IODINE 131; METHYL IODIDE; THICKNESS; VELOCITY

CONTENTS

1. INTRODUCTION

When assessing the hazards arising from atmospheric releases of fresh fission products, iodine-131 is almost always the critical nuclide, owing to the volatility of its compounds and its biological specificity. The hazards arising from other radioactive aerosols or vapours are usually several orders of magnitude lower than those from the iodine isotopes, of which those due to the 131 isotope are the most important.

At low mass concentrations, a large fraction of the iodine may be converted to organic iodide vapour, predominantly methyl iodide. This compound is much more difficult to trap than other forms of airborne radioiodine, especially at high humidity. A number of impregnated charcoals have been developed in Britain and the USA to cope with this problem. Absorption beds of these materials, preceded by high efficiency particulate filters, are capable of removing all forms of airborne radioiodine (or any other fission product, except the inert gases) even at high humidity.

Charcoal beds deteriorate in use and even, occasionally, in storage, becoming poisoned by stray atmospheric contaminants, the concentrations of which may vary widely from place to place, or from time to time. Periodic checks on performance in trapping methyl iodide must be made to ensure that the bed is replaced before the performance at high humidity falls to an unacceptable value. It is rarely possible to control either the temperature or the humidity in an *in situ* test; such tests are usually performed at ambient temperature and a humidity within the range 40 to 70 per cent relative humidity (RH). To partly compensate for the reduced sensitivity that this entails, the tests may be performed, if possible, at a higher flowrate than normal. Temperature variations within the ambient range are not thought to have much effect on charcoal performance, apart from the secondary effects on the relative humidity; a change of 1°C may cause a change in relative humidity of up to 5 per cent. Thus, to translate the results of an *in situ* test into a figure for the expected minimum performance under the worst possible conditions, it is desirable to know how the performance varies with both humidity and face velocity. Such information would also be useful when designing absorption systems, or comparing alternative supplies of charcoal which have been tested under different conditions.

Three batches of impregnated 8/12 mesh 207 B charcoal, manufactured by Sutcliffe, Speakman and Company Limited, UK, were tested for their ability to remove methyl iodide vapour under a wide range of humidity and flowrate conditions. One batch was impregnated with 5 per cent triethylenediamine

(TEDA) and the other two with 1.5 per cent potassium iodide.

2. METHOD

2.1 Test Apparatus

A controlled humidity sampling chamber was developed in which four charcoal samples could be tested simultaneously, either in dry air or in humid air, within the range 30 ± 0.3 per cent RH to 95 ± 1 per cent RH, at a temperature of 26.7 ± 0.2°C. A later version of the chamber (Mark II) could test two samples at humidities up to 99.5 ± 0.3 per cent RH at 26.67 ± 0.02°C.

A sample consisted of a series of densely packed beds, each bed being about 2.4 cm deep, except for the first which was often subdivided into five smaller beds, each about 0.40 cm deep (Figure 1). Each bed was filled with an accurately measured weight of charcoal, so that in any test the variation in depth of the individual beds would be negligible. However, since the density of the charcoal could vary slightly with the prevailing humidity, there might have been variations of a few per cent in the individual bed depth from experiment to experiment, but this was not detected.

The total flowrate through the samples was 2×10^{-3} $m^3 s^{-1}$ (6.67×10^{-4} $m^3 s^{-1}$ for the Mark II version), which could be equally divided between the samples or, more usually, the flow could be divided in the ratios 6:3:2:1 (3:1 in the Mark II). This corresponded to superficial face velocities of approximately 100, 50, 33.3 and 16.7 cm s^{-1} (50 and 16.7 cm s^{-1}) which covered the range of interest in the design of practical absorption equipment.

Figure 2 is a schematic diagram of the apparatus. Dried oil-free compressed air was passed into the humidifier, which could be bypassed if dry air was required. In the humidifier, the air flowed upwards through a bed of Raschig rings through which was passed a counterflow of water from the first control bath. The emerging air was saturated with water vapour at the temperature of the control bath, which could be varied over the range from 8°C to 28.5°C (8°C to 26.9°C), by means of a thermostatically controlled heater and supplementary cooler. This permitted the operator to select the desired humidity of the sampling chamber, after allowance was made for the drop in pressure between the humidifier and the chamber.

The humid air passed through lines, heated just sufficiently to prevent condensation, to a heat exchanger situated within the thermal enclosure. Water at 26.7°C was supplied to the heat exchanger from a second thermostatically controlled bath. The air passed from the heat exchanger over an electrical hygrometer monitoring the humidity, to a Teflon mixing nozzle,

where the iodine was injected, before passing into the lower arm of a star-shaped sampling chamber constructed of 8 cm diameter glass pipe. The four side-arms contained the test samples in quickly demountable holders (Figure 2).

The air was drawn through the samples by vacuum pumps exhausting to a fume cabinet. The sampling chamber was maintained at a slight positive pressure by supplying a small excess of humid air (2-3 per cent) to the chamber and allowing the surplus to escape to the fume cabinet through a charcoal trap in the upper arm of the chamber.

The sampling chamber and some ancillary equipment were mounted on a small insulated trolley, which formed the base of the thermal enclosure. In the Mark I version, a removable plastic hood, 60 cm square by 120 cm deep, was used to cover the sampling chamber and formed the upper part of the thermal enclosure. The temperature of the air inside the enclosure was thermostatically maintained at about 26.7°C. To aid the temperature control of the apparatus, the laboratory was maintained at approximately 24°C by air conditioning.

In the Mark II version, the size of the thermal enclosure was increased to 90 cm square by 2 m deep. It was fully insulated with polystyrene foam and double glazing, so that heat losses and the associated temperature gradients within the enclosure would be reduced to a minimum. The air was continuously stirred by two 10-watt electrical fans, and two more fans were switched on intermittently to provide the heat input for thermostatic control. Two smaller coolers, placed downstream of the two fans in continuous operation, reduced the minimum heat input to the enclosure, permitting the enclosure to be operated close to the ambient temperature which, in turn, kept the temperature gradients to a minimum. Varying the temperature of the refrigerated water supplied to the coolers provided a coarse control to compensate for seasonal variations in laboratory temperature. Temperature control within the enclosure was better than ± 0.02°C.

The pressure at the humidifier outlet was monitored by a manometer and an adjustable mercury pressure switch, which automatically shut down the equipment if the pressure rose above or fell below the operating limits.

2.2 Test Procedure

The flow through each sample was checked against calibrated flowmeters before insertion in the sampling chamber. After a short period to allow the chamber to reach operating temperature, the flow of humid air was started and maintained for at least 17 hours to allow the adsorption of water vapour on the charcoal to reach equilibrium. The work by Wilhelm (1968) suggests

that this period is adequate.

Methyl iodide, labelled with iodine-131, was injected into the mixing nozzle of the sampling chamber, using the apparatus shown in Figure 3 and a method devised by Hilary, Gate & Gurney (1967). Iodine-131 as carrier-free iodide in dilute caustic soda, stabilised with sodium thiosulphate, was dispensed into one arm of the W-tube and mixed with the required amount of stable iodide, normally 10 µg. The usual volume of aqueous solution was from 1 to 3 cm^3. One cm^3 of dimethyl sulphate was placed in the other arm of the W-tube and the iodine released by passing 7 $cm^3 s^{-1}$ of nitrogen through the tube to mix the contents and purge the volatile methyl iodide as it formed. A radiation monitor was used to check the progress of the release, which was invariably almost exponential with time. Injection periods varied from 30 to 60 minutes, by which time over 99 per cent of the iodine had been released. To check for desorption, four similar samples were purged for varying periods, ranging from 15 minutes to 48 hours from the mean injection time. No evidence of any movement of activity under extended purging was found in either dry or humid air, so the usual purge period was restricted to about one hour.

The charcoal in each individual bed of a sample was mixed thoroughly and counted in a known geometry in a calibrated gamma counter. The activity, if any, penetrating the final bed in the sample was estimated from the distribution of activity on the preceding beds. This was necessary only for tests performed at high humidity and is possible only because the deep penetration appears to be exponential in every case. The correction was never more than 2 per cent of the total activity.

3. RESULTS

A total of 238 samples of charcoal, in three separate batches, were tested over a three-year period. The average number of beds in each sample was about seven (varying from a minimum of 2 to a maximum of 15) which makes it essential to summarise the results for presentation.

Figure 4 is a plot of penetration against bed depth for one of the samples tested in dry air and clearly shows the salient features of a typical penetration curve. The penetration into the deeper regions of the bed falls off exponentially with increasing depth, but the leading edge of the bed is less efficient, as if there is a band of charcoal at the leading edge which plays no part in the adsorption process. The thickness of this 'Dead Band', α, is obtained by extrapolation of the exponential part of the curve back to the intercepts at 100 per cent penetration. The other characteristic length required to define each penetration curve is the slope of the line, given here

as the 'Tenth Thickness', β, which is the extra depth of charcoal required to reduce the penetration by a factor of ten.

The penetration for depths greater than about four times the dead band is then given by the formula,

$$\gamma = 10^{-\left(\frac{x-\alpha}{\beta}\right)}, \qquad \ldots(1)$$

where γ is the fractional penetration and x is the depth of charcoal.

A computer program was written to calculate α and β, in which a least squares fit was applied to those points on the exponential part of the curve, with each point weighted inversely proportional to the variance of the counting statistics, by the method given by Bevington (1969). The results of this program were usually in excellent agreement with those in which the curve had been fitted by eye.

Tables 1, 2 and 3 summarise the results for batches A, C and D respectively, giving the computer results for α and β derived from the raw experimental data, which were obtained at the listed face velocities and relative humidities. The column headed ε is discussed in Section 4.4.

4. DISCUSSION OF RESULTS

4.1 Stay Time

Collins, Taylor & Taylor (1967) suggested that the performance of a charcoal bed for methyl iodide at a given humidity was directly proportional to the volume of the charcoal in the bed divided by the volumetric flowrate through the bed, which they called the 'Stay Time'.

Figure 5 is a plot of penetration against stay time for a single test at 94 per cent RH. It can be seen that, although the logarithm of the penetration for each sample falls on a straight line when plotted against stay time, the results for samples tested at different face velocities fall on separate lines, none of which pass through the origin. Moreover, in tests at lower humidities the spread of results is even greater. All the later tests, including those at 99 per cent RH, confirm that the concept of stay time does not give an accurate comparison between charcoals tested at different flowrates and, at low face velocities, could lead to an underestimate by as much as a third in the depth of charcoal required for a given performance at high humidity. At low humidities the discrepancy would be even greater, which would make it very difficult to use the stay time concept to interpret *in situ* tests.

4.2 Dead Band Thickness

There appears to be no correlation between dead band thickness, α, and

humidity or mass of methyl iodide generated, at least up to mg quantities. This rules out the possibility of the effect being due to the bed becoming saturated with methyl iodide. There is some correlation between face velocity and α, but the relation is not a simple one, since the spread of results is much larger than can be attributed to experimental error alone.

The dead band effect had previously been observed on a silvered molecular sieve by Wilhelm (1969), who suggested that it was caused by changes in relative humidity of the almost saturated air, due to expansion in passing through the bed. This cannot be the case, however, since the effect persists, even in dry air.

At first it was thought that the phenomenon might be an aerodynamic effect connected with the buildup of turbulence within the bed. This hypothesis was tested in run A14, where sample number 1 was immediately preceded by an inert bed of 8/12 mesh grit, but there was no significant difference between this sample and the control.

Poisoning (*i.e.* the permanent occupation of the active sites on the charcoal by the chemisorbed molecules of some abundant interfering vapour) had not been seriously considered, since it was thought that the quantity of such vapour in the test atmosphere would be too small for saturation effects to be observed. However, very large dead bands were observed in the first three tests performed on the KI-impregnated charcoal of batch C and poisoning was immediately suspected. That the poisoning was connected with the change in charcoal and not a change in the operating conditions was confirmed by reverting to the TEDA-impregnated charcoal of batch A.

A poisoning test (A23) was performed to try to identify the cause. The results of this test were not absolutely clear, since batch A was not nearly so sensitive as batch C, but it did suggest that dimethyl sulphate vapour might be responsible.

To test this supposition, a caustic soda bubbler was inserted in the nitrogen line from the methyl iodide generator to trap dimethyl sulphate vapour without affecting the release of the methyl iodide. In subsequent tests, the dead bands for both batch A and batch C were about half those previously observed for batch A and an order of magnitude less than those in C1-3. This is strong evidence in favour of poisoning being the cause of the dead band effect.

It was considered that the small residual dead bands were probably due to poisoning of the charcoal by traces of the plasticiser from the tubing of the sampling chamber. There is additional evidence that dioctylphthalate,

which is commonly used as a plasticiser and as a test aerosol for particulate filters, may be a charcoal poison.

It is noted that the size of the dead bands tended to increase with the number of tests performed. This was probably due to progressive fouling of the caustic soda trap with dimethyl sulphate, leading to a loss of efficiency of the trap.

4.3 Tenth Thickness

Tenth thickness, β, was found to be a function of both face velocity and relative humidity but independent of iodine carrier level. Figures 6, 7 and 8 are logarithmic plots of β *versus* face velocity for batches A, C and D respectively, omitting the three poisoned runs of batch C.

There is considerable scatter in the experimental points, but the points for any given humidity appear to lie around straight lines. There seem to be no significant differences between Figures 6 and 8, and Figure 7 is similar to the other two figures, except that the values of β are about 20 per cent greater. It was decided, therefore, to use a statistical approach to determine the correlation between the parameters. The results from batch C and batch D would be incorporated in the assessment of batch A by multiplying the values of β by appropriate conversion factors.

A computer program was written to determine the lines of least squares fit for each group of points at similar humidities for various values of the conversion factors, covering a range of about 6 per cent either side of the likely values. The conversion factors giving the optimum values of the average standard deviation for all common humidities (*i.e.* 94, 80, 50 and 30 per cent RH) were 0.99 for batch D and 0.83 for batch C. The conversion factors are a direct measure of the relative trapping efficiencies compared to batch A.

The solid lines in Figures 6, 7 and 8 are the lines of least squares fit, using these values to combine all three batches, for each group of points close to a common humidity. The intercept, A, at a face velocity V = 1 m s^{-1} (log V = 0) and the slope of the line, B, were determined for the combined batches and a correlation was sought with humidity. Straight lines were obtained when either log A (Figure 9) or B (Figure 10) was plotted against the percentage relative humidity, h, provided the figures for dry air were omitted.

This means that the correlation between β, V and h, for the range of practical interest, *i.e.* 30-99 per cent RH and 1.1 m s^{-1} to 0.16 m s^{-1}, is given by

$$\beta = P.e^{r.h}.V^{(s+t.h)} \quad , \qquad \ldots(2)$$

where log P is the intercept at h = 0, and r is the slope of the line of least squares fit in Figure 9, s is the intercept at h = 0, and t is the slope in Figure 10. The values of the correlation coefficients of the lines of least squares fit for Figures 9 and 10, and the values of P, r, s and t are given in Table 4, for the three batches of charcoal.

4.4 Data Scatter

The experimental deviation, ε (defined as the difference between the values of β, found by experiment and predicted from formula 2, expressed as a percentage of the predicted value), was calculated for each experimental point and is given in column 7 of Tables 1, 2 and 3. Examination of ε suggests that formula 2 gives the slope of the penetration curve with a standard deviation of 7 per cent over a humidity range of 30-99 per cent RH, and a velocity range of at least 6 to 1 and possibly as much as 170 to 1. It is surprising that this empirical relationship appears to hold down to less than 7 mm s^{-1}, since the formula suggests that the effect of humidity on the slope reverses at velocities less than 3 mm s^{-1}, which throws doubt on the validity of the formula at very low velocities.

It is disappointing that the scatter in the results should be so high, especially in view of the precision with which most of the penetration curves fit an exponential curve, (Figures 4 and 5). Possible reasons for the scatter were investigated, such as poisoning of the charcoal during storage, variations in temperature of the Mark I sampling chamber leading to changes in the relative humidity, uncertainty in the measurement of the flowrate, and even variations in the depth of charcoal due to changes in the weight of water vapour adsorbed; but all these effects are too small, by factors of about 3 or more, to explain the observed scatter.

The increased scatter at very low humidities can be explained by the poor statistics of a few of the results before the introduction of the subdivided first bed.

An explanation for a major portion of the scatter may be variations in the charcoal itself. The degree of activation, the mean size of the granules, and the amount of inert foreign matter present in the charcoal would all play a part in varying the trapping efficiency. The difficulty of reproducing the precise characteristics of a type of charcoal is illustrated by the differences between batches C and D, both of which were supplied by the manufacturer at the same time in separate drums, yet reputed to be of the same batch. There

was a marked difference in bulk density which, though unexpected, was readily detected (batch D was 12 per cent lighter than batches C and A) and a marked difference in trapping efficiency (batch C was about 20 per cent inferior to batches D and A). The observed scatter could be explained by smaller differences than this, if they occurred within the batch and the mixing techniques were inadequate.

5. *IN SITU* TESTING

To translate the result of an *in situ* test of a charcoal bed, performed at a humidity h per cent RH and a face velocity of V_1 m s^{-1}, into an expected performance at 100 per cent RH and a face velocity of V_2 m s^{-1}, let the observed penetration be 10^{-y} and the depth of the bed be x, the dead band thickness (or poisoned region) be α and the tenth thickness at h per cent RH be β_1. Then from Formula 1:

$$y = \frac{x-\alpha}{\beta_1}$$

or

$$x-\alpha = y.\beta_1 \quad . \qquad \ldots(3)$$

Let the penetration at 100 per cent RH and normal face velocity be 10^{-z} and the tenth thickness be β_2. Then from Formula 1:

$$z = \frac{x-\alpha}{\beta_2} \quad ,$$

from Formula 3

$$z = y.\beta_1/\beta_2 \quad ,$$

and from Formula 2

$$z = \frac{y.P.e^{r.h}.V_1^{(s+t.h)}}{P.e^{100r}.V_2^{(s+100t)}} \quad ,$$

which reduces to

$$z = y.e^{r(h-100)}.(V_1/V_2)^s.V_1^{t.h}.V_2^{-100t} \quad . \qquad \ldots(4)$$

If the test is performed at the normal face velocity V, this expression reduces to

$$z = y.e^{r(h-100)}.V^{t(h-100)} \quad . \qquad \ldots(5)$$

Note that the depth of the bed, the depth of the poisoned region, and the batch variable, P, do not appear in Formulas 4 and 5.

6. CONCLUSION

The penetration of methyl iodide was found to be exponential with bed depth in the deeper regions of the charcoal bed. The slope of this portion of the penetration curve was dependent upon both the face velocity and the relative humidity in a more complex manner than the simple relationship suggested by the stay time concept. An empirical formula, which gave the slope of the penetration curve within a standard deviation of 7 per cent, was derived to correlate the parameters over the range of practical interest, *i.e.* 30-99 per cent RH and 1.1 m s^{-1} down to 0.16 m s^{-1} and possibly much lower. The degree of uncertainty in the results may be attributable to variations in quality within the individual batches of charcoal.

At the leading edge of the bed was a band of charcoal, whose performance had been affected by poisoning agents in the airstream drawn through the bed. This poisoned region could be expected to grow during the working life of the bed, until the performance at high humidity had fallen to the point which made replacement necessary.

In situ tests should be carried out periodically to check on the performance. A formula was derived to translate the observed performance into the expected performance at high humidity and any other flowrate. The expression is independent of the slope of the penetration curve and the thicknesses of both poisoned and unpoisoned regions of the bed, which suggests that it may be valid even for heavily poisoned beds. Confirmation of this, however, must await the development of non-destructive tests.

7. REFERENCES

Bevington, P.R. (1969) - Data Reduction and Error Analysis for the Physical Sciences. McGraw-Hill Book Co.

Collins, D.A., Taylor, L.R. & Taylor, R. (1967) - The Development of Impregnated Charcoals for Trapping Methyl Iodide at High Humidity. UKAEA TRG Report 1300 (W).

Hillary, J.J., Gate, L.F. & Gurney, K. (1967) - Experience in Testing Installed Fission Product Trapping Plant with Methyl Iodide. UKAEA TRG Report 1548 (W).

Wilhelm, J.G. (1968) - Testing Iodine Filters for Nuclear Installations. Symp. on Operating and Developmental Experience in the Treatment of Airborne Radioactive Wastes, New York, 26-30 August. IAEA, Vienna pp.403-16.

Wilhelm, J.G. (1969) - Trapping of Fission Product Iodine with Silver Impregnated Molecular Sieves. KFK 1065.

TABLE 1

RESULTS FOR BATCH A

8/12 MESH 207 B + 5% TEDA

Run No.	Humidity % RH	Sample No.	Face Velocity* cm s^{-1}	α mm	β mm	ε %	Comment
A3	95	1	50.3	3.8	43.0	- 5	
A4	95	1	51.0	2.7	42.6	- 7	48 h purge
		2	49.8	2.6	43.7	- 3	15 min purge
		3	50.3	2.7	43.9	- 3	6 h purge
		4	50.3	2.8	43.3	- 4	15 min purge
A5	80	1	17.3	0.0	15.7	- 4	
		2	30.7	2.8	22.0	- 9	
		3	50.2	4.6	31.7	- 6	
		4	103.2	9.1	56.2	+ 3	
A6	80	1	17.8	- 0.0	16.0	- 4	
		2	32.8	1.9	22.8	- 10	
		3	49.7	2.9	31.2	- 7	
		4	100.8	7.2	53.6	- 1	
A7	60	1	17.7	- 0.0	11.8	- 3	
		2	33.0	0.7	17.6	- 1	
		3	49.0	3.6	22.2	- 1	
		4	101.7	9.0	34.9	+ 1	
A8	49.5	1	17.5	- 0.0	9.9_1	- 4	
		2	33.0	0.6	14.1	- 4	
		3	49.5	3.6	17.9	- 2	
		4	101.3	6.3	27.2	- 1	
A9	94	1	17.5	0.5	19.0	- 8	
		2	33.2	1.8	30.2	- 8	
		3	49.2	3.3	41.7	- 5	
		4	101.5	7.3	73.4	- 1	
A11	< 1	1	49.3	2.0	8.5_8	+ 21	34 min purge
		2	50.2	1.4	10.4	+ 46	5.5 h purge
		3	51.3	2.1	8.9_7	+ 25	24 h purge
		4	50.2	- 0.0	9.4_1	+ 32	48 h purge
A12	< 1	1	16.6	0.7	5.3_0	+ 12	
		2	33.7	2.0	7.4_3	+ 21	
		3	50.2	4.1	8.7_5	+ 23	
		4	101.0	7.3	12.3	+ 33	
A13	< 1	1	16.8	0.6	5.5_3	+ 16	
		2	33.0	1.4	7.9_6	+ 30	
		3	50.2	1.8	9.7_7	+ 37	
		4	101.3	5.9	13.9	+ 50	
A14	< 1	1	50.0	4.0	12.2	+ 71	turbulence test
		2	50.7	3.6	12.7	+ 77	control sample
A15	< 1	1	17.3	0.5	6.7_3	+ 40	
		2	34.0	0.7	11.1	+ 80	
		3	50.7	3.5	10.1	+ 41	
		4	100.7	9.8	13.1	+ 42	
A16	< 1	1	17.3	1.0	5.6_2	+ 17	
		2	34.0	1.2	9.5_2	+ 54	
		3	50.7	5.7	11.1	+ 55	
		4	100.7	8.5	12.6	+ 37	
A17	< 1	1	17.3	0.9	5.7_0	+ 18	
		2	34.0	1.6	9.1_7	+ 48	
		3	50.7	1.8	9.3_5	+ 31	
		4	100.7	5.0	12.4	+ 34	
A18	94	1	17.2	1.0	20.5	+ 1	
		2	33.0	3.1	32.1	- 2	
		3	49.3	5.0	43.6	0	
		4	101.8	9.8	79.2	+ 7	
A19	94	1	17.3	0.3	20.0	- 2	
		2	33.2	1.4	31.7	- 3	
		3	50.3	3.5	42.0	- 5	
		4	107.3	9.3	74.7	- 3	
A20	30	1	17.2	0.4	7.9_1	+ 5	
		2	33.3	1.9	11.0	+ 6	
		3	50.0	5.6	11.3	- 10	
		4	100.8	7.9	17.6	0	
A21	30	1	17.0	1.0	7.1_2	- 5	
		2	32.8	- 0.0	10.5	+ 2	
		3	49.3	4.3	12.1	- 3	
		4	102.0	10.5	16.9	- 5	
A22	75	1	0.667	- 0.00	2.03	+ 12	
A23	50	1	49.3	3.6	19.1	+ 3	Poisoning test
		2	50.0	7.0	18.7	0	
		3	50.7	5.8	19.6	+ 4	
		4	51.3	3.5	19.1	+ 1	
A24	50	1	16.8	0.1	9.4_1	- 7	Caustic soda trap in line in all subsequent tests.
		2	33.5	0.5	15.6	+ 5	
		3	51.2	0.9	18.5	- 2	
		4	99.8	3.3	28.2	+ 3	
A25	50	1	17.0	0.0	10.3	+ 1	
		2	33.8	0.8	15.4	+ 3	
		3	50.3	1.4	18.3	- 2	
		4	100.2	6.5	28.3	+ 3	
A26	50	1	17.0	- 0.0	10.5	+ 3	
		2	33.8	0.7	16.3	+ 9	
		3	50.3	1.4	20.3	+ 9	
		4	100.3	5.4	29.5	+ 7	
A27	50	1	16.8	- 0.0	10.0	- 1	
		2	33.3	0.6	16.7	+ 12	
		3	50.2	1.4	20.4	+ 9	
		4	101.0	5.3	29.4	+ 7	

* *A correction is applied to the face velocity calculations to account for the total activity found on each sample in a run.*

TABLE 2

RESULTS FOR BATCH C

8/12 MESH 207 B + 1.5% KI

Run No.	Humidity % RH	Sample No.	Face Velocity* cm s^{-1}	α mm	β mm	ε %	Comments
C1	94	1	16.5	⩾ 1.6	⩽ 24.8	+ 4	
		2	33.3	⩾ 4.0	⩽ 41.0	+ 3	Poisoned by
		3	50.5	⩾ 10.7	⩽ 52.5	- 2	dimethyl
		4	101.0	⩾ 13.1	⩽103.1	+ 16	sulphate
C2	50	1	17.0	⩾ 3.6	⩽ 15.4	+ 25	vapour to
		2	34.2	⩾ 5.8	⩽ 25.1	+ 38	which this
		3	50.8	⩾ 13.1	⩽ 29.4	+ 30	charcoal is
		4	99.5	⩾ 16.1	⩽ 56.0	+ 70	very sensitive
C3	50	1	16.6	⩾ 6.2	⩽ 14.3	+ 18	
		2	32.7	⩾ 7.0	⩽ 23.7	+ 34	
		3	51.2	⩾ 17.6	⩽ 26.9	+ 18	
		4	101.0	⩾ 16.4	⩽ 52.8	+ 59	
C4	50	1	16.7	- 0.1	12.3	+ 1	Caustic soda
		2	33.8	0.0	19.2	+ 6	trap in line
		3	50.2	2.3	24.4	+ 8	
		4	100.7	2.8	38.3	+ 15	
C5	50	1	16.7	- 0.1	13.1	+ 8	
		2	33.5	0.1	19.6	+ 9	
		3	49.3	3.3	24.1	+ 8	
		4	101.8	4.1	38.2	+ 14	
C6	50	1	16.8	- 0.1	13.5	+ 10	
		2	33.5	0.5	19.4	+ 8	
		3	49.7	5.6	23.7	+ 6	
		4	101.3	4.0	39.4	+ 18	
C7	94	1	16.7	- 0.0	22.2	- 7	
		2	33.3	0.7	37.5	- 5	
		3	49.5	4.8	47.9	- 9	
		4	101.8	4.9	84.7	- 5	
C8	94	1	16.7	- 0.0	22.1	- 8	
		2	33.5	0.9	36.8	- 8	
		3	49.7	3.4	48.5	- 9	
		4	101.7	5.3	82.4	- 8	
C9	94	1	16.8	0.1	21.9	- 9	
		2	34.0	0.8	36.4	- 10	
		3	49.8	2.3	48.2	- 9	
		4	100.7	3.3	83.8	- 5	

Run No.	Humidity % RH	Sample No.	Face Velocity* cm s^{-1}	α mm	β mm	ε %	Comments
C10	80	1	16.8	0.1	18.6	- 4	
		2	34.2	0.8	30.1	- 4	
		3	50.0	3.1	37.7	- 7	
		4	100.3	5.7	64.8	0	
C11	80	1	16.8	- 0.0	18.2	- 6	
		2	33.8	1.1	29.6	- 5	
		3	49.8	2.2	37.9	- 6	
		4	100.8	5.1	64.7	0	
C12	80	1	17.0	0.2	18.1	- 7	
		2	33.7	1.3	30.3	- 2	
		3	50.0	3.9	39.0	- 4	
		4	100.7	6.9	65.5	+ 1	
C13	30	1	17.2	- 0.1	9.07	0	
		2	34.3	0.1	13.5	+ 7	
		3	50.0	- 0.0	16.5	+ 9	
		4	100.0	4.3	22.0	+ 4	
C14	30	1	16.8	0.0	8.64	- 4	
		2	34.0	0.4	13.4	+ 6	
		3	49.3	1.0	13.9	- 8	
		4	101.2	5.7	19.6	- 8	
C15	30	1	17.0	- 0.1	8.33	- 8	
		2	33.8	0.0	12.6	0	
		3	50.3	3.1	14.3	- 6	
		4	100.3	5.2	19.6	- 8	
C16	94	1	16.3	0.9	24.5	+ 4	
		2	33.5	2.3	41.0	+ 3	
		3	50.3	5.5	54.1	+ 1	
		4	112.5	10.9	104.2	+ 8	
C17	80	1	16.8	1.7	19.2	- 1	
		2	33.8	3.5	32.6	+ 5	
		3	49.8	8.2	38.0	- 6	
		4	100.7	16.7	64.1	- 1	
C18	80	1	16.5	1.1	20.2	+ 5	
		2	34.0	3.6	30.7	- 2	
		3	49.8	8.0	36.7	- 9	
		4	101.0	14.9	62.7	- 4	
C19	80	1	17.0	1.2	17.4	- 11	
		2	34.0	2.9	28.1	- 10	
		3	50.2	2.2	33.6	- 17	
		4	100.2	11.3	56.7	- 12	

* *A correction is applied to the face velocity calculations to account for the total activity found on each sample in a run.*

TABLE 3

RESULTS FOR BATCH D

8/12 MESH 207 B + 1.5% KI

Run No.	Humidity % RH	Sample No.	Face Velocity* cm s^{-1}	α mm	β mm	ε %	Comments
D0	94	1	16.5	0.5	19.1	- 4	
		2	33.7	1.7	30.2	- 10	
		3	49.8	3.2	40.4	- 9	
		4	101.2	8.1	64.6	- 13	
D1	94	1	16.7	0.9	18.7	- 7	
		2	33.3	2.2	32.9	- 1	
		3	49.8	3.6	44.1	- 1	
		4	101.5	10.0	71.7	- 4	
D2	94	1	16.5	1.3	19.2	- 4	
		2	33.5	2.8	32.9	- 1	
		3	49.8	4.3	45.4	+ 2	
		4	101.5	12.5	73.1	- 2	
D3	80	1	16.7	0.5	13.9	- 14	
		2	33.3	2.0	22.8	- 12	
		3	49.7	1.1	31.3	- 7	
		4	101.7	7.3	49.5	- 10	
D4	80	1	16.7	0.6	14.9	- 8	
		2	33.5	2.2	22.8	- 12	
		3	49.8	2.5	32.0	- 5	
		4	101.3	8.3	50.9	- 7	
D5	80	1	16.8	0.8	15.1	- 7	
		2	33.7	2.6	23.0	- 12	
		3	50.3	4.2	31.3	- 8	
		4	100.7	10.6	48.1	- 12	
D6	50	1	16.8	- 0.0	10.0	- 2	
		2	33.7	0.7	14.8	- 2	
		3	49.8	0.5	18.9	+ 1	
		4	100.8	4.9	26.8	- 4	
D7	50	1	16.8	0.8	9.5_7	- 7	
		2	33.8	1.6	15.4	+ 2	
		3	50.2	3.9	18.4	- 3	
		4	100.7	7.5	27.1	- 3	
D8	50	1	16.6	0.3	10.9	+ 7	
		2	33.3	2.0	15.1	+ 1	
		3	50.2	4.6	18.4	- 3	
		4	101.3	8.4	28.3	+ 1	
D9	50	1	16.5	0.5	10.3	+ 2	
		2	33.3	2.2	15.1	+ 1	
		3	49.8	3.4	20.1	+ 7	
		4	101.5	8.8	28.5	+ 2	
D10	30	1	16.7	0.8	8.2_2	+ 9	
		2	33.7	1.7	11.5	+ 9	
		3	50.2	3.9	13.6	+ 7	
		4	100.7	9.5	18.0	+ 1	
D11	30	1	16.7	- 0.1	8.6_5	+ 15	
		2	33.5	0.8	11.3	+ 8	
		3	50.0	1.4	13.3	+ 5	
		4	101.2	3.2	18.9	+ 6	
D12	30	1	16.5	0.2	7.7_0	+ 3	
		2	33.3	1.0	11.4	+ 9	
		3	49.8	3.0	13.8	+ 9	
		4	101.5	8.5	17.6	- 2	
D13	94	1	16.5	0.2	21.0	+ 5	
		2	33.5	1.3	34.5	+ 3	
		3	49.8	1.7	49.6	+ 11	
		4	101.3	10.0	77.3	+ 4	
D14	94	1	16.8	0.3	21.8	+ 8	Mark II thermal enclosure
		2	50.3	2.8	49.1	+ 9	
D15	99	1	16.8	0.8	23.2	+ 6	
		2	50.3	4.2	51.7	+ 4	
D16	99	1	16.8	1.2	24.2	+ 11	
		2	50.3	4.7	55.0	+ 11	
D17	99	1	16.8	0.8	24.0	+ 10	
		2	50.3	4.9	51.4	+ 4	
D18	99	1	16.8	1.1	23.5	+ 8	
		2	50.3	2.5	54.6	+ 10	
D19	99	1	16.8	0.4	22.6	+ 4	
		2	50.3	3.2	50.4	+ 2	
D20	99	1	16.8	1.1	24.1	+ 11	
		2	50.3	4.2	53.0	+ 7	
D21	98	1	16.8	1.0	23.3	+ 8	
		2	50.3	3.3	51.6	+ 6	
D22	98	1	16.8	1.7	24.7	+ 15	
		2	50.3	4.0	59.1	+ 22	

* *A correction is applied to the face velocity calculations to account for the total activity found on each sample in a run.*

TABLE 4

VALUES OF CONSTANTS IN FORMULA 2

(Derived from lines of least squares fit in Figures 9 and 10)

Constant	Batch A	Batch C	Batch D	Correlation Coefficient
p	9.0 ± 0.5 mm	10.8 ± 0.5 mm	9.1 ± 0.5 mm	0.9964
r		$(2.2_3 \pm 0.08) \times 10^{-2}$ per % RH		
s		$(3.6_5 \pm 0.21) \times 10^{-1}$		0.9840
t		$(3.8_6 \pm 0.29) \times 10^{-3}$ per % RH		

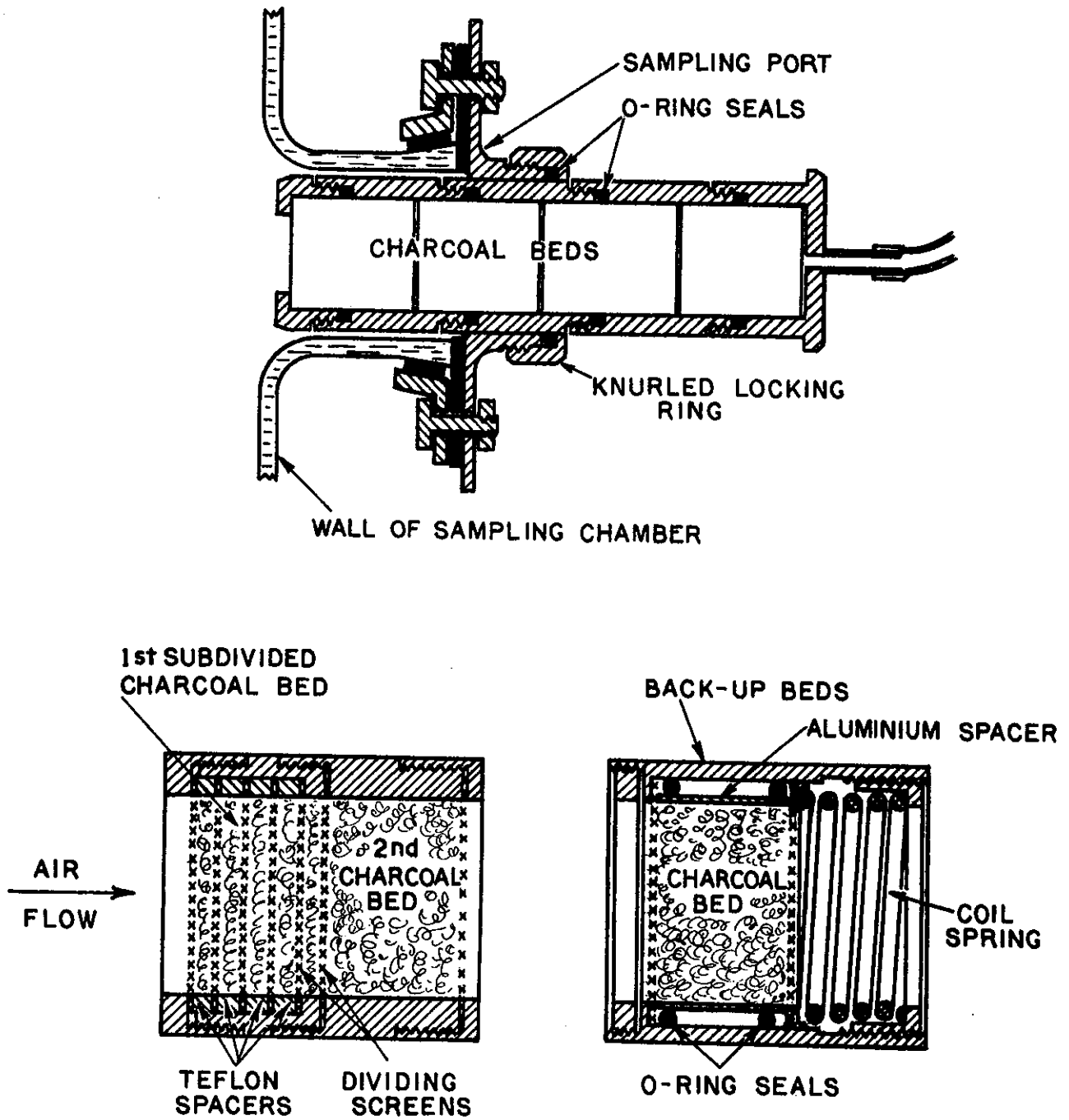

FIGURE 1. DETAILS OF CHARCOAL BEDS AND SAMPLING PORT

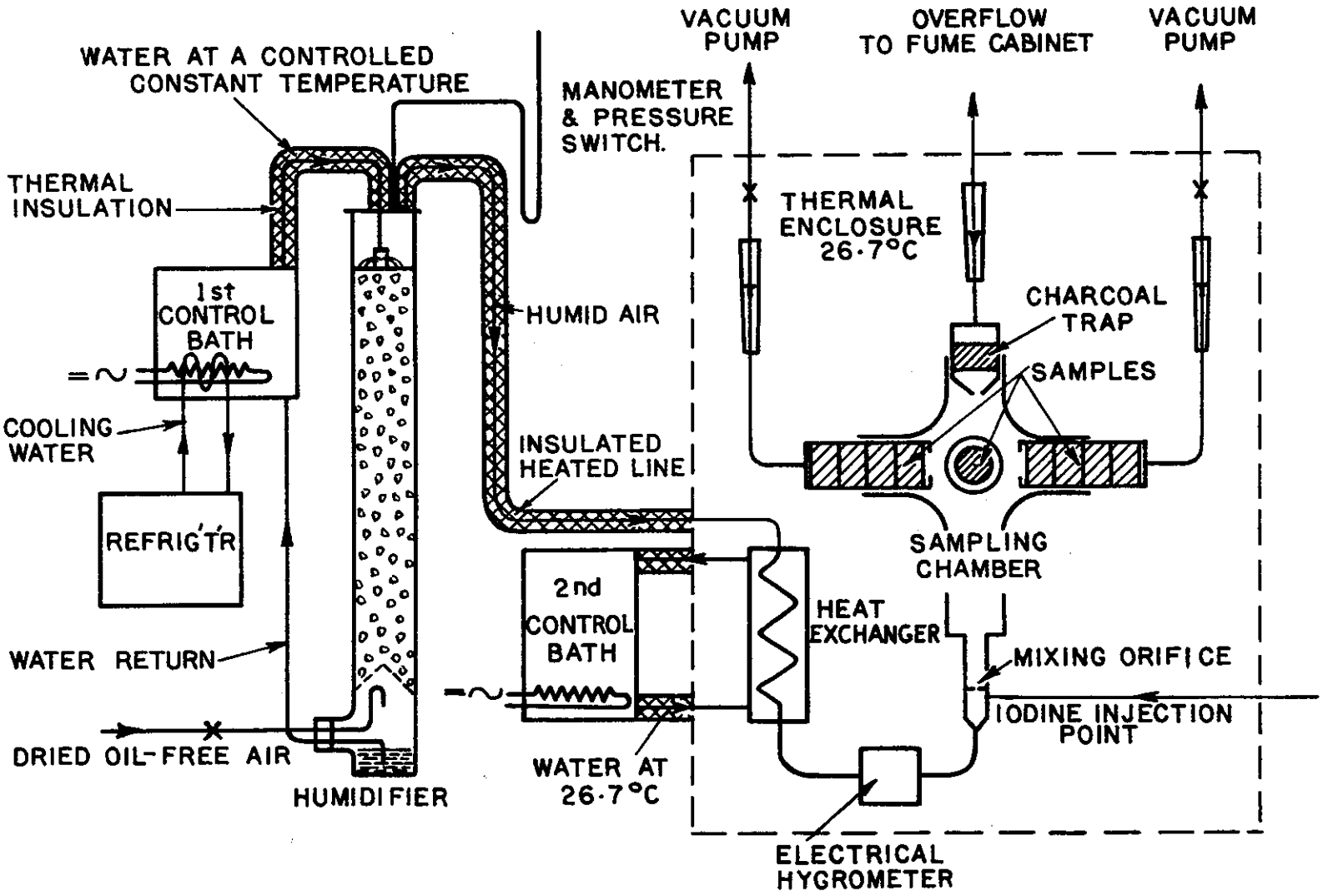

FIGURE 2. SCHEMATIC DIAGRAM OF APPARATUS

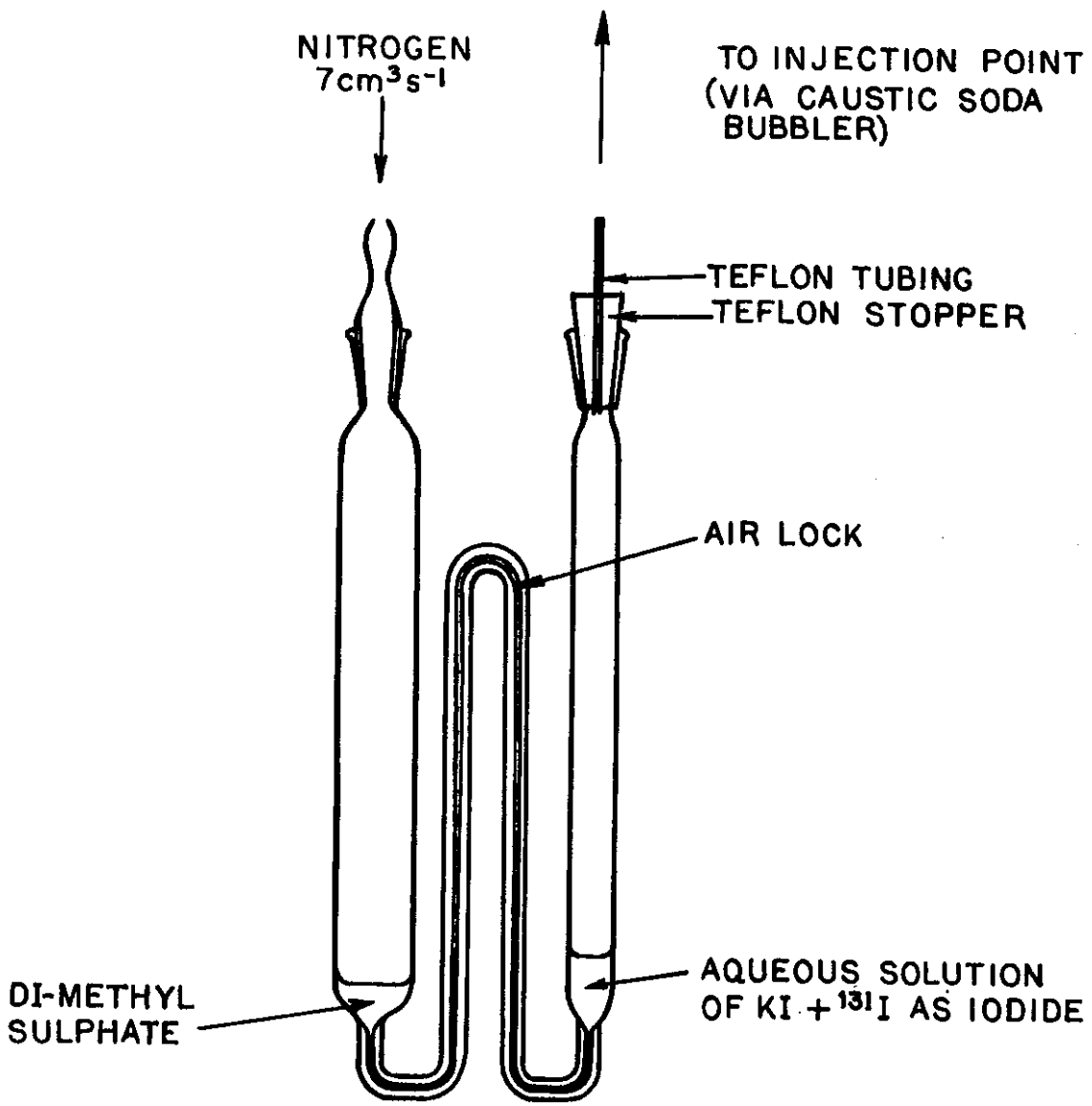

FIGURE 3. METHYL IODIDE GENERATOR

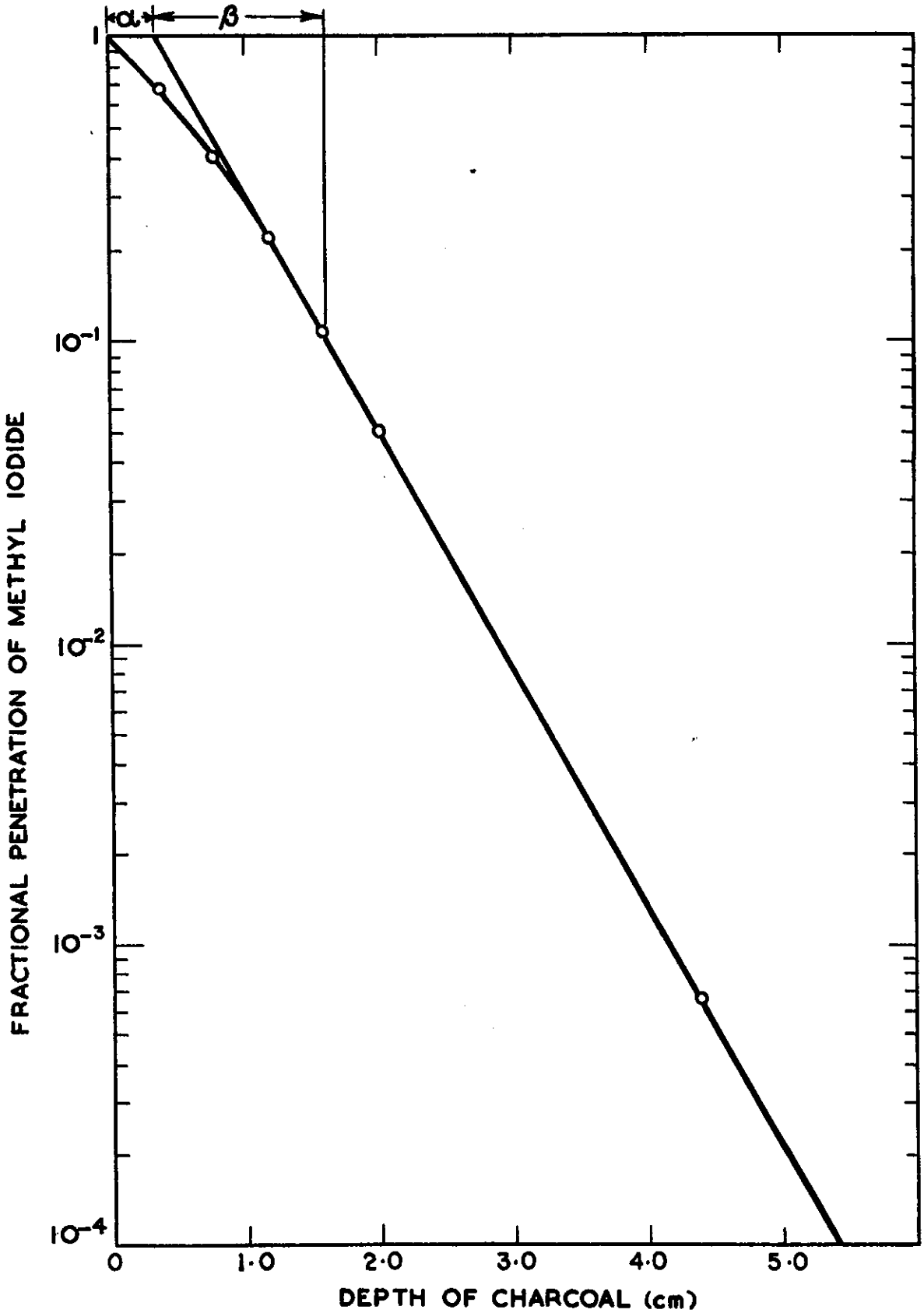

FIGURE 4. TYPICAL PENETRATION CURVE

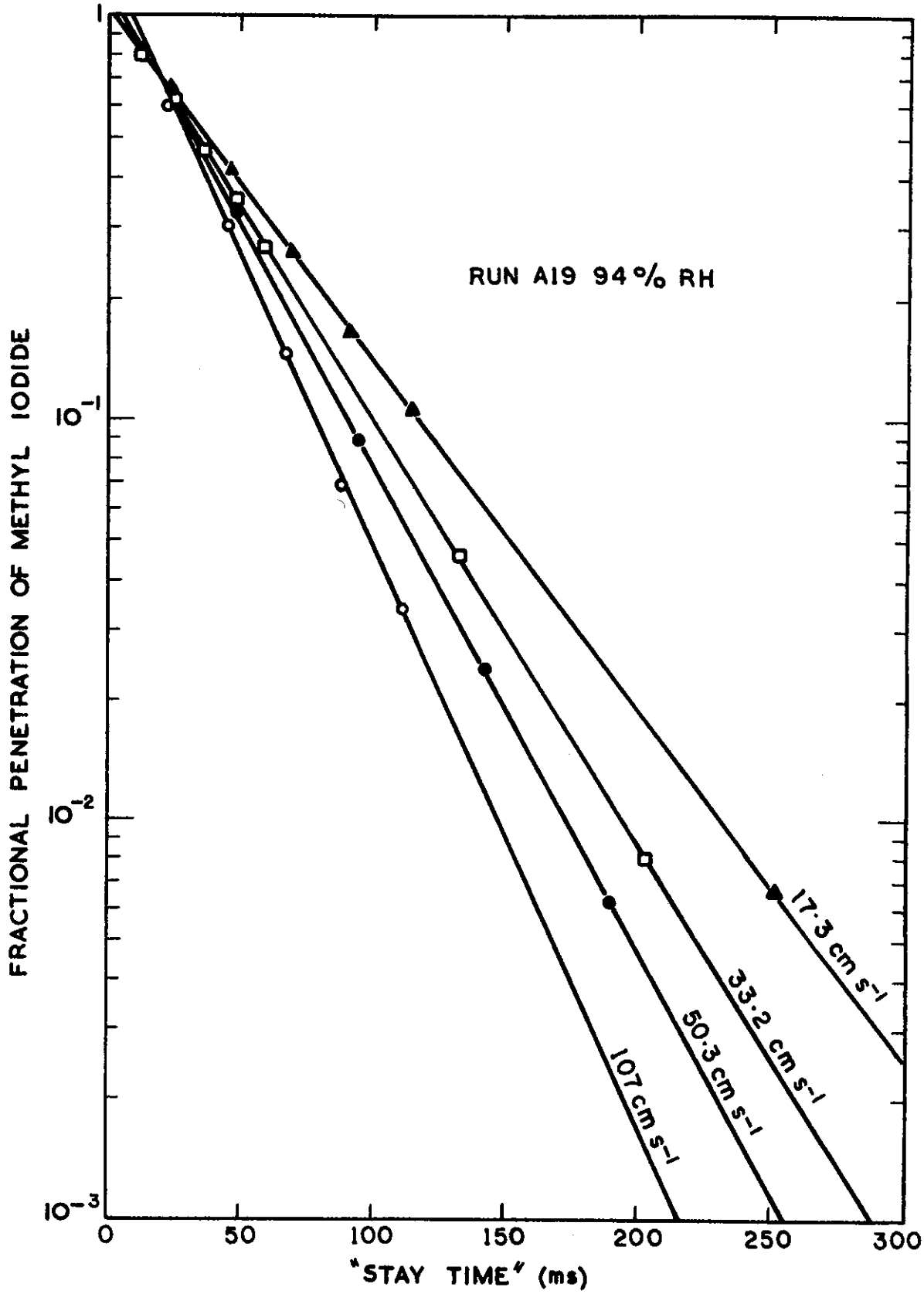

FIGURE 5. PLOT OF PENETRATION AGAINST 'STAY TIME'

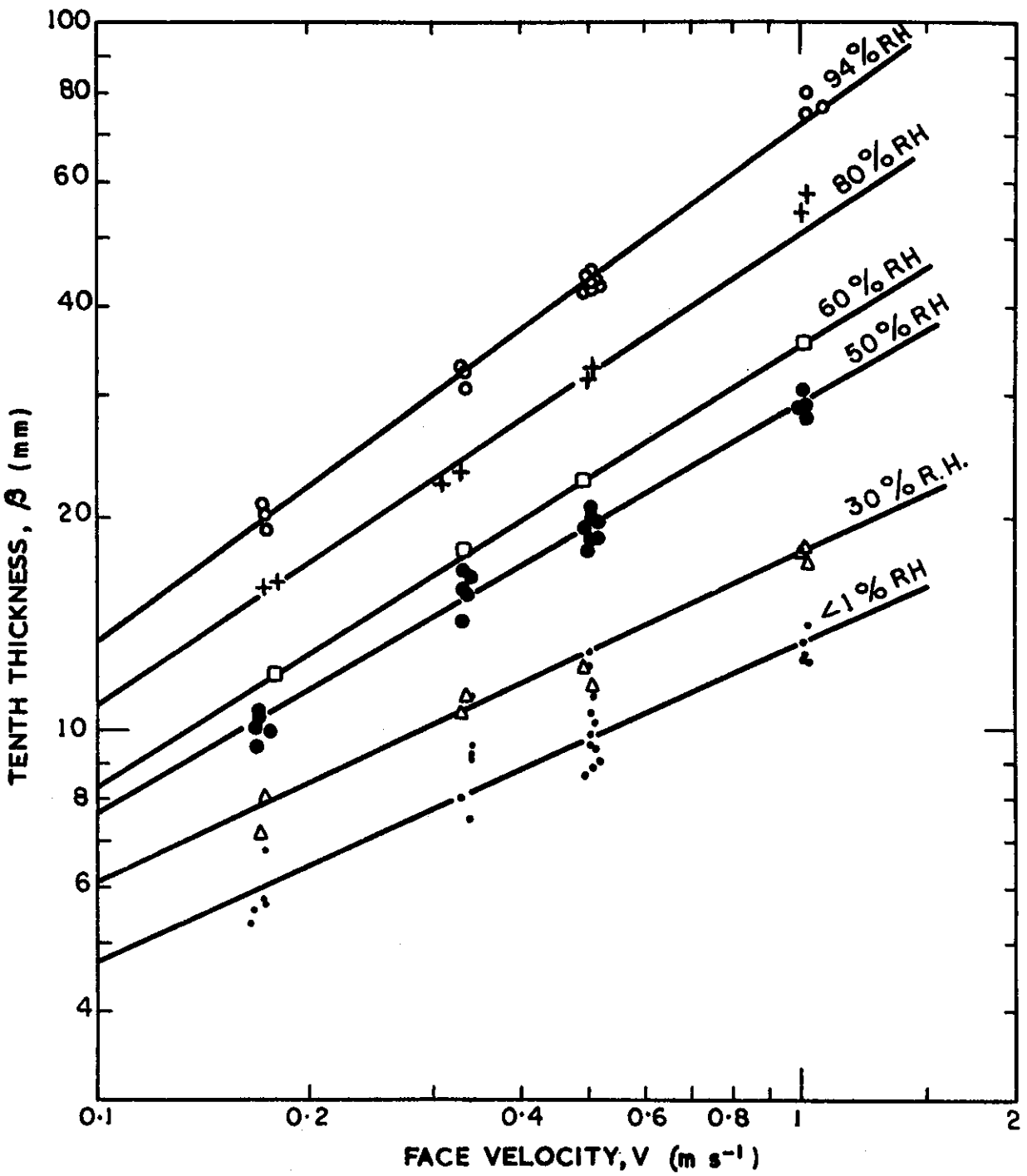

FIGURE 6. VARIATION OF TENTH THICKNESS WITH FACE VELOCITY FOR BATCH A

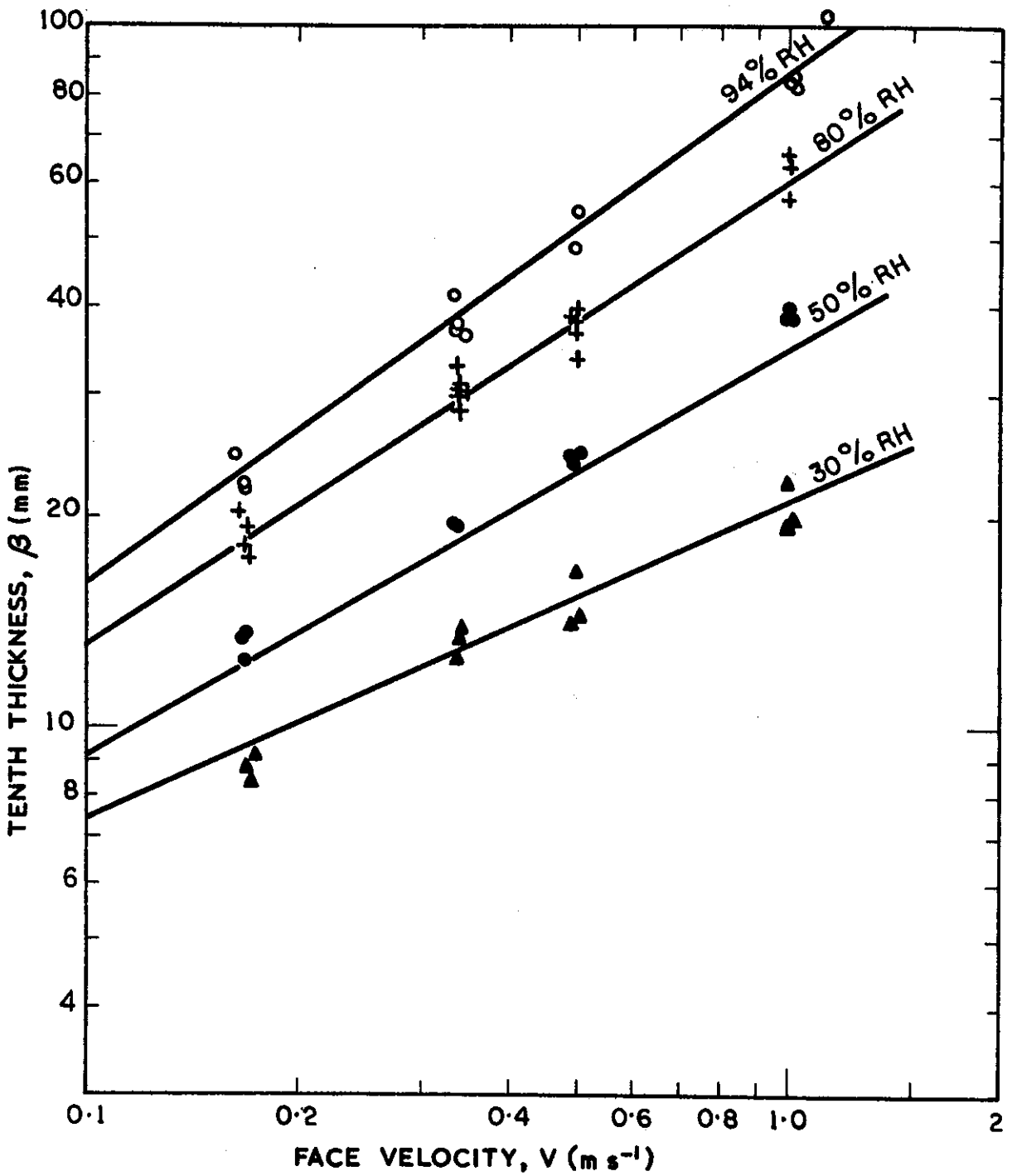

FIGURE 7. VARIATION OF TENTH THICKNESS WITH FACE VELOCITY FOR BATCH C

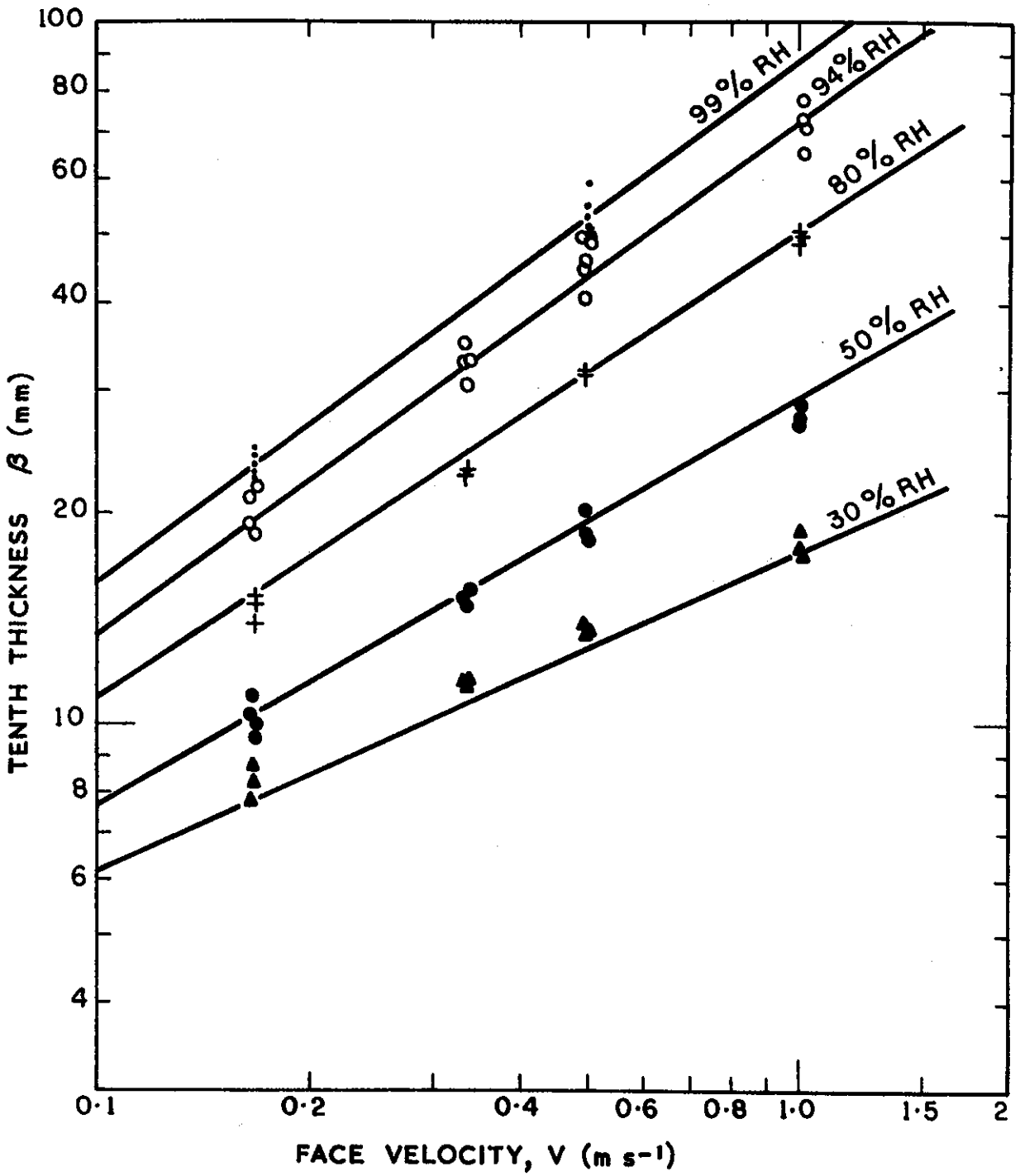

FIGURE 8. VARIATION OF TENTH THICKNESS WITH FACE VELOCITY FOR BATCH D

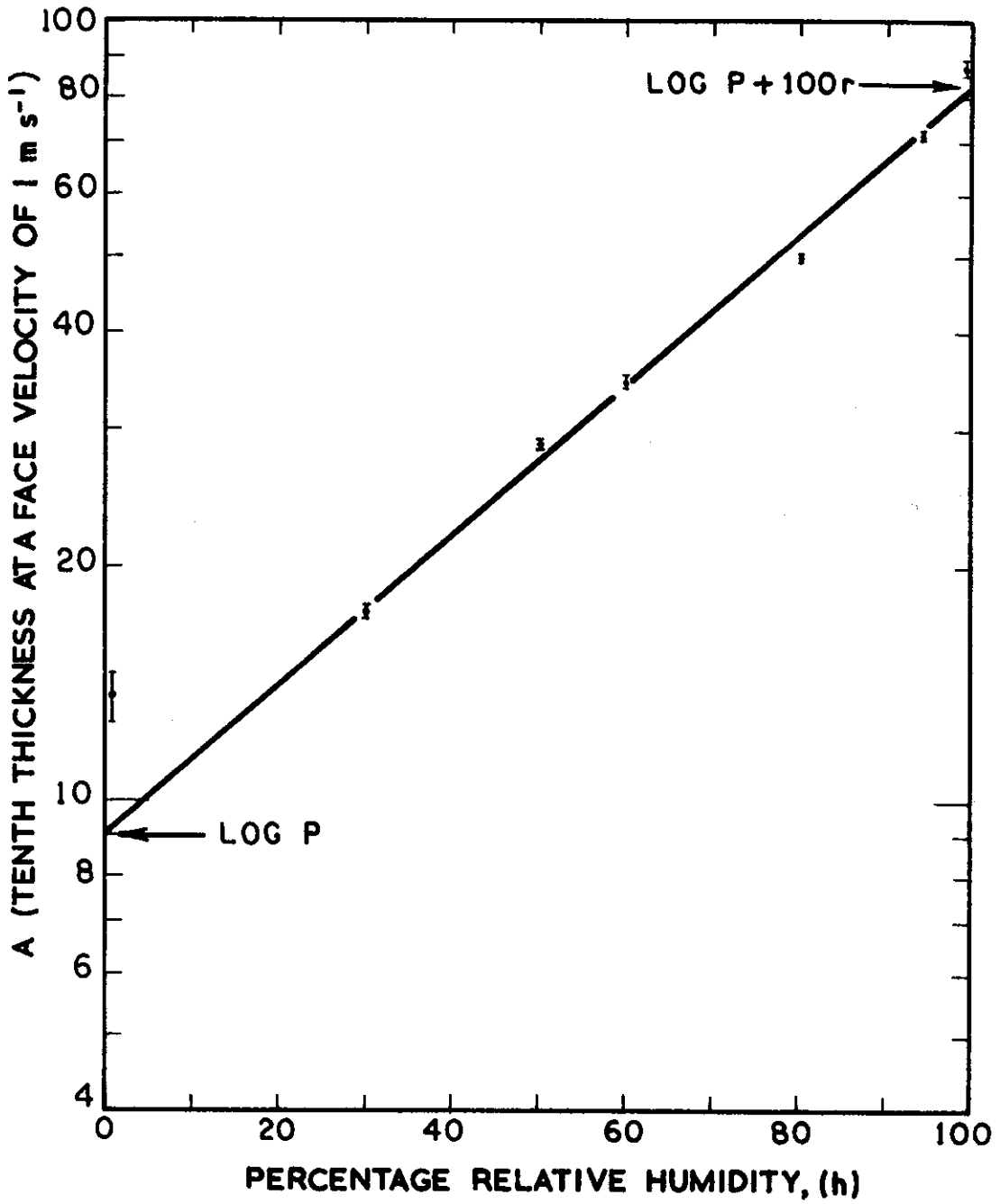

FIGURE 9. PLOT OF THE INTERCEPT A (FROM FIGURES 6 AND 8) AGAINST RELATIVE HUMIDITY

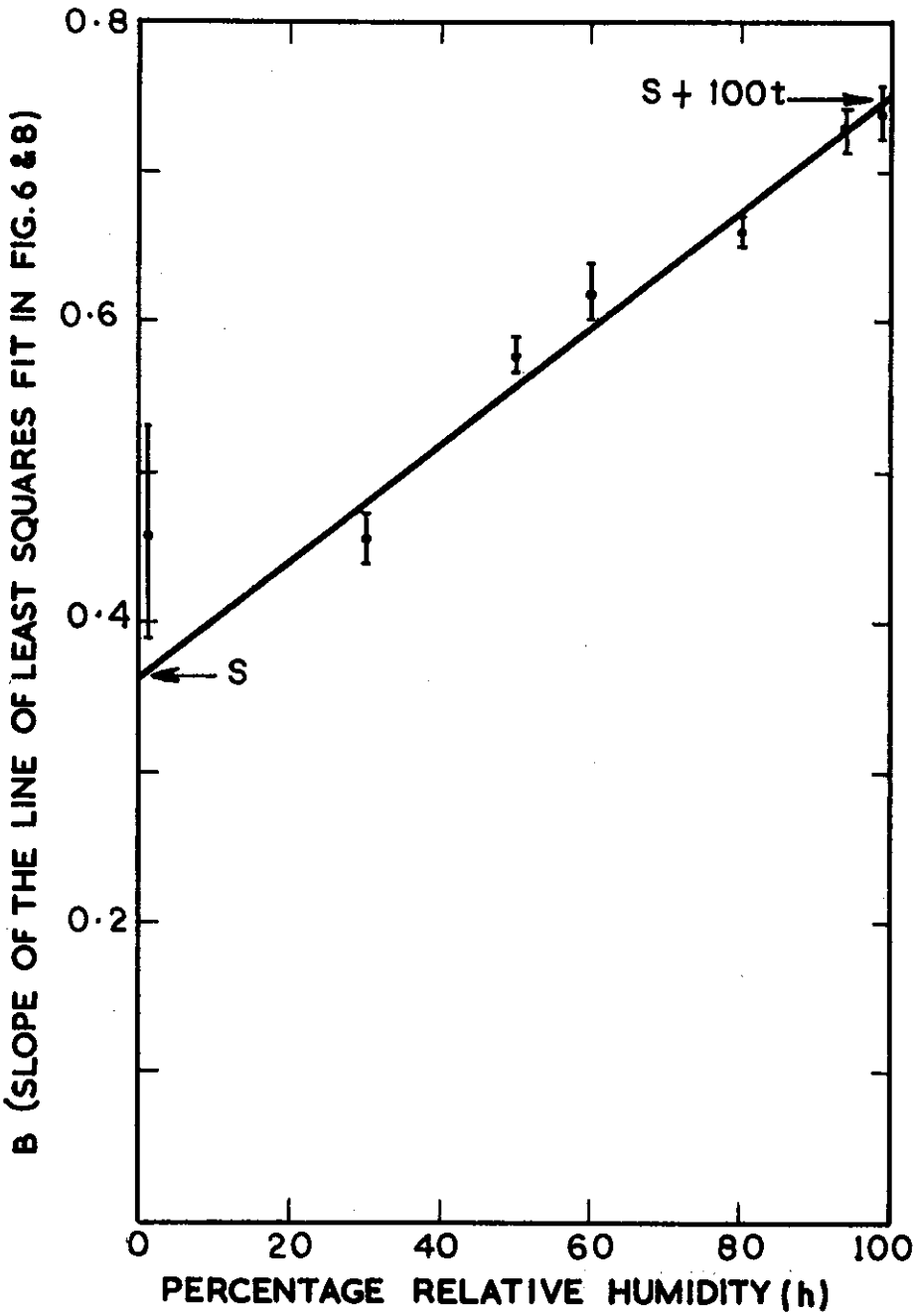

FIGURE 10. PLOT OF SLOPE OF LINE B (FROM FIGURES 6 AND 8) AGAINST RELATIVE HUMIDITY